

Effect of *Vitreoscilla* Hemoglobin Dosage on Microaerobic *Escherichia coli* Carbon and Energy Metabolism

Philip S. Tsai, Vassily Hatzimanikatis, and James E. Bailey*
Institute of Biotechnology, ETH, CH-8093 Zürich, Switzerland

Received March 23, 1995/Accepted August 7, 1995

The amount of *Vitreoscilla* hemoglobin (VHb) expression was modulated over a broad range with an isopropyl- β -D-thiogalactopyranoside- (IPTG-) inducible plasmid, and the consequences on microaerobic *Escherichia coli* physiology were examined in glucose fed-batch cultivations. The effect of IPTG induction on growth under oxygen-limited conditions was most visible during late fed-batch phase where the final cell density increased initially linearly with increasing VHb concentrations, ultimately saturating at a 2.7-fold increase over the VHb-negative (VHb⁻) control. During the same growth phase, the specific excretions of fermentation by-products, acetate, ethanol, formate, lactate, and succinate from the culture expressing the highest amount of VHb were reduced by 25%, 49%, 68%, 72%, and 50%, respectively, relative to the VHb⁻ control. During the exponential growth phase, VHb exerted a positive but smaller control on growth rate, growth yield, and respiration. Varying the amount of VHb from 0 to 3.8 $\mu\text{mol/g}$ dry cell weight (DCW) increased the specific growth rate, the growth yield, and the oxygen consumption rate by 33%, 35%, and 60%, respectively. Increasing VHb concentration to 3.8 $\mu\text{mol/g}$ DCW suppressed the rate of carbon dioxide evolution in the exponential phase by 30%. A metabolic flux distribution analysis incorporating data from these cultivations discloses that VHb⁺ cells direct a larger fraction of glucose toward the pentose phosphate pathway and a smaller fraction of carbon through the tricarboxylic acid cycle from acetyl coenzyme A. The overall nicotinamide adenine dinucleotide [NAD(P)H] flux balance indicates that VHb-expressing cells generate a net NADH flux by the NADH/NADPH transhydrogenase while the VHb⁻ cells yield a net NADPH flux under the same growth conditions. Flux distribution analysis also reveals that VHb⁺ cells have a smaller adenosine triphosphate (ATP) synthesis rate from substrate-level phosphorylation but a larger overall ATP production rate under microaerobic conditions. The thermodynamic efficiency of growth, based on reducing equivalents generated per unit of biomass produced, is greater for VHb⁺ cells. © 1996 John Wiley & Sons, Inc.

Key words: *Vitreoscilla* hemoglobin • flux analysis • dose response • microaerobic metabolism

INTRODUCTION

Escherichia coli, a microbe capable of switching between multiple metabolic networks for energy generation, thrives on energetically most favorable pathways in a particular

environment. When cells are grown aerobically with glucose as carbon and energy substrate, glucose is efficiently dissimilated into cellular materials. Metabolic energy is generated in the form of proton motive force across the cytoplasmic membrane with concomitant recycling of redox carriers using oxygen as an exogenous electron acceptor. In the absence of oxygen, energy synthesis depends on substrate-level phosphorylation, and redox reactions are balanced internally by decomposition of glucose into wasteful metabolites which are then excreted into the environment.

The biochemistry and genetics of both aerobic and anaerobic pathways in *E. coli* are now well understood and characterized. Unfortunately, in most industrial bioprocesses involving *E. coli* or other microorganisms, problems arise mostly, not with aerobiosis or anaerobiosis, but with microaerobiosis in which aspects of both respiration and fermentative metabolisms are active and rival for accomplishing energy synthesis and redox balance. During microaerobic conditions, environmental factors such as nonideal mixing result in fluctuations of culture dissolved oxygen (DO) tension between hypoxic and anoxic.^{22,27} Internally, global and specific oxygen regulation mechanisms activate and repress key enzymes to prepare cells for aerobic or anaerobic survival.^{12,29} Accordingly, the product pattern changes dramatically during microaerobiosis.²⁶

It has been demonstrated, through genetic engineering, that intracellular expression of a bacterial hemoglobin from *Vitreoscilla* (VHb) into different hosts elicits in vivo effects of reduced oxygen starvation, improved cell growth, and product formations.^{7,15,18,21} Recent studies aimed at understanding the mechanism of VHb action indicate that VHb increases the number of protons extruded across the cytoplasmic membrane per oxygen atom reduced and enhances the adenosine triphosphatase- (ATPase-) catalyzed ATP synthesis rate in microaerobic *E. coli*.^{5,14} Kallio et al.¹⁴ suggest that VHb improves the electron transport chain through a catalytic role in raising the activity of the terminal oxidase cytochrome *o*. Given the intricate interactions between respiratory and fermentative metabolisms under microaerobic conditions, a perturbed respiratory pathway could have an effect on central carbon metabolism and the flux distribution. Unfortunately, the effect of VHb on carbon metabolism as well as effect of VHb dosage on physiological responses are unknown for any of the organisms reported. Studying these consequences of VHb expression

* To whom all correspondence should be addressed.

will enhance understanding of interactions of Vhb with microaerobic physiology. This will expand the foundation of information useful in guiding future applications of Vhb technology.

Models that predict intracellular flux distribution and its perturbation as a result of enzymatic or environmental manipulations have been developed and applied in different organisms in recent years.^{8,28} Straightforward yet informative methods such as stoichiometric flux balancing analysis, which demands knowledge only on biochemical stoichiometry, biosynthesis requirements, and a few measurable parameters, find increasing applications in metabolic engineering.^{11,30,35} Based on experimental data, this mass balancing method interprets the observed physiology by providing a quantitative analysis of flux distribution within the defined network of reactions.

In this work we addressed the two previously posed questions of (1) how microaerobic *E. coli* physiology responds to Vhb dosage and (2) how Vhb perturbs microaerobic *E. coli* carbon and energy flux distributions. We compared different growth parameters and by-product excretion patterns of six Vhb-expressing *E. coli* cultures under oxygen-limited conditions. Using the gathered information a metabolic flux distribution model based on stoichiometric balancing of *E. coli* glucose metabolism was applied, and the effect of Vhb on flux distribution was studied. Based on this information, the implications of Vhb expression on microaerobic physiology and indications concerning the mechanism of Vhb action were discussed.

MATERIALS AND METHODS

Microorganism, Plasmid Construction, and Cultivation Conditions

The effects of different intracellular Vhb concentrations on cell physiology was studied using *Escherichia coli* K-12, strain W3110¹ transformed with the isopropyl- β -D-thiogalactopyranoside- (IPTG-) inducible Vhb expression plasmid, pKTV1. Plasmid pKT1 was constructed by digesting pBR322⁴ with *EcoRI* and *SspI* and ligating with the 1.1-kb *EcoRI*-*HindIII* fragment [*HindIII*-digested fragment posttreated with DNA polymerase I large (Klenow) fragment (Promega Inc.)] containing the *lac* repressor gene, *lacI^q*, from pMJR1560 (Amersham International). Plasmid pKTV1 was then created by subcloning the 1.2-kb *HindIII*-*SalI* fragment containing the *tac* promoter-*vhb* gene fusion from pINT1¹⁶ into the corresponding sites in pKT1. Different levels of Vhb expression were achieved by varying doses of IPTG. Ampicillin (100 mg/L) was added to all W3110:pKTV1 cultivations for plasmid maintenance.

Seeding cultures for bioreactor cultivations were grown for 12 h in 500-mL shake flasks containing 100 mL of buffered Luria-Bertani (LB) medium (10 g/L Bactotryptone, 5 g/L Bacto-yeast extract, 10 g/L NaCl, 3 g/L K₂HPO₄, 1 g/L KH₂PO₄, adjusted to pH 7) at 37°C and 250

rpm in a New Brunswick Scientific Innova 4000 shaker. Glucose fed-batch cultivations were performed in a Six Fors bioreactor (Infors, AG) with working volume of 310 mL. Bioreactor cultivations were inoculated with 6.2 mL of seed culture, and process parameters were maintained at 37°C, pH 7 (adjusted with either 3 M NaOH or 3 M H₃PO₄), 400 rpm, and 0.4 vvm (volume of gas per volume of liquid per minute) of air supply. Glucose-defined batch medium consisted of 4 g/L glucose, 0.4 g/L (NH₄)₂SO₄, 4.35 g/L K₂HPO₄, 1.5 g/L KH₂PO₄, 1 mL/L trace metal mix (8.3 mM Na₂MoO₄, 7.6 mM CuSO₄, 8 mM H₃BO₃), 1 mL/L vitamin mix (0.042% riboflavin, 0.54% panthothenic acid, 0.6% niacin, 0.14% pyridoxin, 0.006% biotin, 0.004% folic acid), 1 mM MgSO₄, 0.05 mM CaCl₂, 0.2 mM FeCl₃, and 100 mg/L ampicillin.

Induction of Vhb was achieved by adding the indicated concentration of IPTG to the culture when dissolved oxygen (DO) dropped below 5% of air saturation, which generally occurred approximately 10 h postinoculation. The fed-batch mode was commenced with 1 mL/h of feed medium when the culture reached an A₆₀₀ of 1.5 and 2 mL/h when A₆₀₀ reached 3.0. Thereafter the feeding was kept constant at 2 mL/h until the end of cultivation.

Feed medium consisted of 250 g/L glucose, 110 g/L (NH₄)₂SO₄, 8 g/L MgSO₄, 1 mL/L vitamin mix, 1 mL/L trace metal mix, 0.05 mM CaCl₂, and 0.2 mM FeCl₃. DO was monitored with a pO₂ electrode (Ingold, Inc.) and exhaust gas (CO₂ and O₂) from the bioreactor was monitored using an emission monitor (Brüel & Kjaer, Emissions Monitor type 3427). Samples for Vhb, total protein, and excreted metabolite measurements were taken periodically throughout cultivations and stored at -20°C until analysis.

Analytical Procedures

Metabolite analyses for formate, D-lactate, L-lactate, succinate, and pyruvate were performed enzymatically as described by Bergmeyer.^{2,3} Assays were performed at 37°C on a Beckman SYNCHRON CX5CE autoanalyzer by coupling reactions to NAD(P) and following changes in NAD(P)H at 340 nm ($\epsilon_{\text{NAD(P)H}} = 6.22 \text{ cm}^{-1} \text{ mM}^{-1}$). Biochemicals and enzymes were of analytical grade and were obtained from Boehringer Mannheim or Sigma. Acetate concentration was measured with a gas chromatograph (Hewlett-Packard 5890 series II with a flame ionization detector) with a Carbovac CW 20 M 0.25 (25 m \times 0.25 mm) column. Gas chromatography (GC) analysis was performed on a three-ramp oven temperature program: the initial temperature was held at 70°C for 1 min, then the temperature was raised 10°C/min to 95°C, thereafter the temperature was increased to 131°C with a rate of 40°C/min, and then to 190°C with a rate of 70°C/min where it was maintained for 4 min. The detector and the inlet temperatures were 300°C and 220°C, respectively; helium and nitrogen gas flow rates were 1 and 100 mL/min, respectively. Butyric acid, 5 mM, was added as an internal standard to samples for acetate determination. Glucose and ethanol concentrations in cul-

ture medium were measured with glucose (GLU) and ALC assays (Beckman), respectively, using a Beckman SYNCHRON CX5CE autoanalyzer.

Samples for protein assay were prepared by resuspending harvested cells 1:1 in a sonication buffer [100 mM Tris, pH 8; 50 mM NaCl; 1 mM ethylenediaminetetraacetic acid (EDTA), pH 8]. Cells were disrupted by sonication on ice in a sonifier (Branson model 450) under continuous mode for 12 min at 100% output, followed by centrifugation at 4°C, 15,000 rpm, in an Eppendorf centrifuge. Total soluble protein of the supernatant was determined from a M-TP assay (Beckman) using a Beckman SYNCHRON CX5CE autoanalyzer. For dry cell weight (DCW) determination, 10 mL of culture samples were centrifuged at 3000g and washed once with phosphate buffer saline (8 g/L NaCl, 0.2 g/L KCl, 1.44 g/L Na₂HPO₄, 0.24 g/L KH₂PO₄, adjusted to pH 7). Wet pellets were dried in an 80°C oven for 3 days, and then their weights were measured. DCW measurement has an error margin of 5%.

VHb Quantification

The VHb activity was assayed by CO-reduced minus reduced difference absorption spectrophotometry using the monomer extinction coefficient ($\epsilon_{419\text{nm}} - \epsilon_{437\text{nm}}$) of $1.067 \times 10^5 \text{ M}^{-1} \text{ cm}^{-1}$ for VHb.¹⁰ VHb time profiles of different IPTG inductions were monitored and quantified by Western blotting. Fifteen percent sodium dodecyl sulfate–polyacrylamide gel electrophoresis (SDS–PAGE) and the subsequent Western blotting were performed according to the method of Laemmli²⁰ and the standard Western protocol,³⁶ respectively, with rabbit anti-VHb antiserum (Cocalico Biologicals) and horseradish peroxidase-conjugated sheep IgG fraction to rabbit IgG (Cappel™, Organon Teknika Corp.). Using a molecular dynamics densitometer, the amount of VHb in each sample was estimated by comparing the intensity of its Western blot negative with that of a hemoglobin standard (4.5 μM) prepared from *E. coli* JM101:pRED2 cell extract.¹⁵ Hemoglobin content was normalized with DCW and is reported as micromoles per gram DCW.

RESULTS

Controlled Expression of VHb and Its Effect on Growth

Effect of VHb dosage on microaerobic cell physiology was studied with controlled expression of VHb from a medium-copy-number, *tac*-driven VHb expression plasmid pKTV1. A copy of the *lacI^q* gene was also subcloned on this plasmid to ensure an adequate basal level of repressor to prevent *vhb* transcription in the absence of inducer IPTG. Plasmid pKTV1 was transformed into *E. coli* wild-type strain W3110 to obtain the recombinant strain W3110:pKTV1. Different levels of VHb synthesis were achieved by varying

concentration of IPTG added to the culture in the range of 0 to 0.5 mM. To examine the effect of VHb dose under the most relevant physiological conditions, namely microaerobic growth, VHb synthesis was induced only when the culture DO dropped below 5% of air saturation. The maximal level of VHb, judged from antiserum binding to VHb on Western blots, was 3.8 $\mu\text{mol/g}$ DCW after 31 h of fed-batch cultivation (Fig. 1). This level of synthesis is comparable to VHb expression from a pUC-based, high-copy-number plasmid such as pRED2 (ref. 15; result not shown). The data in Figure 1 disclose that accumulation of VHb increased with increasing concentration of IPTG, and no VHb was detected when no inducer was added.

Six different IPTG-induced, glucose fed-batch W3110:pKTV1 fermentations were performed to study the effect of VHb dosage on cell growth (Fig. 2A). The air flow rate was purposely set low at 0.4 vvm so that cultures became microaerobic (DO equal to or below 2% of air saturation) at the beginning of exponential growth. DO profiles of all cultivations were similar, and therefore only one is shown in Figure 2A. After 40 h of growth, the cells with increasing VHb concentrations grew to higher densities than the uninduced, VHb-free cells (Fig. 2a). For clarity of presentation, the six cultures will be identified hereafter by their VHb concentrations measured after 31 h of cultivation. Although it has been demonstrated that the expression of VHb improves microaerobic cell growth,^{15,17} these data show for the first time that the growth enhancement is proportional to VHb concentration up to a saturation level at a VHb concentration of 3.4 $\mu\text{mol/g}$ DCW (Fig. 2A). Beyond 3.4 μmol VHb/g DCW, no further increase in final cell density was observed (Fig. 2B). The final cell density of the highest VHb-expressing culture was 2.7-fold that of the uninduced, VHb-free culture.

From Figure 2A it is apparent that the most notable differences on cell growth among the six cultures occurred, not during the exponential growth phase, but during the late fed-batch phase. The specific growth rate of cells in the

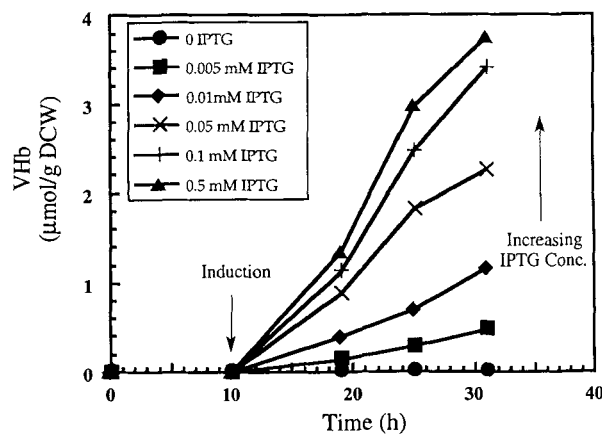


Figure 1. VHb induction pattern of *E. coli* W3110:pKTV1 grown in glucose-defined medium. IPTG was added to culture at hour 10 to induce VHb expression. VHb content of cells, estimated from Western blotting, was normalized with dry cell weight and is reported as $\mu\text{mol/g}$ DCW.

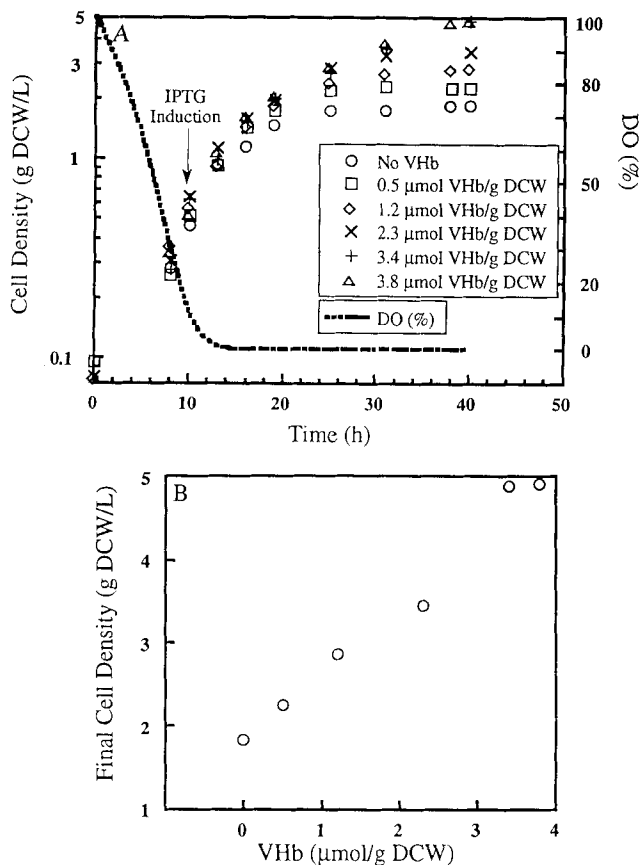


Figure 2. (A) Glucose fed-batch bioreactor growths of W3110:pKTV1 with different Vhb concentrations. Different doses of IPTG (0, 0.005, 0.01, 0.05, 0.1, and 0.5 mM) were added to cultivations at hour 10 to achieve different Vhb expression levels. Dissolved oxygen profiles of the six cultivations were similar and only the representative one is shown. Glucose feeding strategy is described in Materials and Methods (B) Effect of IPTG induction on final cell density.

exponential phase, although also increased with increasing Vhb concentrations, was raised only by 33% from 0.12 h^{-1} without Vhb to 0.16 h^{-1} with 3.8 $\mu\text{mol Vhb/g DCW}$ (Table I). The specific glucose uptake rate remained similar with and without Vhb, and thus the yield on glucose increased with increasing Vhb concentrations (Table I). Sim-

ilar growth patterns and effects of Vhb dosage were observed with repeated cultivations and when W3110:pKTV1 was cultivated in glycerol defined medium under identical conditions (results not shown).

Effect of Vhb Levels on Respiration

The oxygen uptake (OUR, Q_{O_2}) and carbon dioxide evolution (CER, Q_{CO_2}) rates of cells in the exponential phase were calculated from exhaust gas measurements and are summarized in Table I. Although these measurements have an estimated error of around 10%, results showed a significant 60% increase and a 30% decrease in OUR and CER, respectively, of the highest Vhb expressing W3110:pKTV1 relative to the uninduced, Vhb-free control. A closer examination of the data revealed that a small amount of Vhb was sufficient to cause a 30% increase on the respiration rate of *E. coli* W3110:pKTV1; only 0.5 $\mu\text{mol Vhb/g DCW}$ raised OUR from 1.7 to 2.2 mmol $\text{O}_2/\text{g DCW/h}$. Overall, expression of Vhb in the range studied exerted a positive effect on OUR and, to a lesser extent, a negative effect on CER of cells. As a consequence, increasing Vhb decreased the RQ (ratio of CER and OUR). This result suggests that the presence of Vhb may direct microaerobic *E. coli* to utilize more of its respiratory pathways and less of fermentative pathways.

Effect of Vhb Levels on Extracellular Metabolite Concentration

The effect of Vhb dosage on fermentative pathways of *E. coli* was studied by monitoring the production of several important fermentation by-products during cultivations. The use of an automated analyzer improved precision and reduced the uncertainty of assays to about 5 mg/L. Table II summarizes the specific metabolite production of the different IPTG-induced W3110:pKTV1 cultures measured after 31 h of growth. L-lactate concentrations of all cultures were very low and therefore only D-lactate concentrations are reported. Synthesis of Vhb greatly reduced all of the measured metabolites excreted by cells relative to the un-

Table I. Effect of Vhb levels on *E. coli* growth parameters (exponential phase, 13–19 h of cultivation).

Vhb ($\mu\text{mol/g DCW}$)	μ (h^{-1})	$Y_{x/\text{gluc}}$ (mol C/mol C)	mmol/g DCW/h			RQ ^b
			Q_{gluc} ^a	Q_{O_2}	Q_{CO_2}	
0	0.12	0.31	2.61	1.7	2.2	1.3
0.5	0.13	0.31	2.74	2.2	1.8	0.81
1.2	0.13	0.34	2.62	2.5	2.0	0.79
2.3	0.14	0.38	2.47	2.2	1.9	0.88
3.4	0.17	0.41	2.68	2.7	1.8	0.67
3.8	0.16	0.42	2.57	2.7	1.5	0.57

^aCalculated from medium glucose concentration and feedings of 0.25 g/h after culture A_{600} reached 1.5 and 0.5 g/h after A_{600} reached 3.0.

^bRQ = $Q_{\text{CO}_2}/Q_{\text{O}_2}$.

Table II. Metabolite excretion of Vhb-synthesizing *E. coli* in glucose-defined medium (measured after 31 h of cultivation).

Vhb μmol/g DCW	Biomass g DCW/L	Excreted metabolite (mmol/g DCW)					
		Acet	ETOH	Form	D-Lac	Suc	Pyr
0	1.71	62.6	18.7	117	13	6.2	0.06
0.5	2.28	55.3	12.3	64.8	3.8	4.2	0.03
1.2	2.65	56.0	10.1	60.5	3.1	3.3	0.03
2.3	3.24	52.3	10.0	62.4	4.4	2.7	0.03
3.4	3.50	48.5	8.9	37.0	3.7	2.8	0.02
3.8	3.83	47.1	9.5	37.4	3.4	3.2	0.02

induced, Vhb-free control. Vhb has the smallest effect on the repression of acetate production compared with the other metabolites. Increasing Vhb concentrations decreased levels of acetate by a maximal 25% from 62.6 to 47.0 mmol/g DCW over the Vhb concentrations tested.

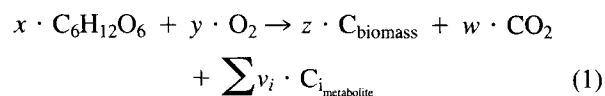
Expression of Vhb had a strong negative effect on formate and D-lactate concentrations as the presence of as little as 0.5 μmol Vhb/g DCW drastically depressed the production of formate and D-lactate by 45% and 70%, respectively. Further increments of Vhb reduced the excretion of formate and D-lactate to 68% and 72%, respectively, of the uninduced W3110:pKTV1 levels. Concentrations of ethanol and succinate were decreased monotonically with increasing Vhb dosage; ethanol and succinate measured from cultures with 3.8 μmol Vhb/g DCW were about 50% of those of the uninduced culture values. Extracellular pyruvate was only measurable toward the end of cultivation where a two- to threefold difference was observed between the uninduced, Vhb-free and the Vhb⁺ cultures (Table II). Because of the small amount of pyruvate detected compared with other metabolites, extracellular pyruvate was excluded from further analyses (except for carbon balance, see below).

Carbon and Redox Balances

To examine whether all the carbon input was accounted for, a carbon balance analysis was performed on each cultivation after 31 h of cell growth. When cells are grown in

minimal media with glucose as the carbon and energy source, the incoming substrate can be recovered in the form of biomass, by-products, and carbon dioxide. Table III shows the distribution of glucose into recovered biomass, excreted metabolites, and evolved CO₂ (from exhaust gas measurement) in millimoles of carbon. Based on cell composition reported by Neidhardt,²³ the cellular carbon content of *E. coli* grown in minimal media can be calculated as 39.8 mmol carbon/g DCW. After summing the glucose input over 31 h of cultivation and multiplying the biomass and metabolite concentrations (in Table II) by their respective carbon contents, the extents of carbon recovery of all W3110:pKTV1 cultures were found to be 93% or higher of the total carbon input.

A redox, or electron, balance was also performed as a consistency check for the carbon balance and, in addition, to cross-examine the accuracy of our CER measurement since it potentially carries the largest error (10%) of all assays reported in this study. For the electron balance, the net metabolic reactions of cells grown on glucose as the sole substrate can be expressed in millimoles of carbon as follows:



where x , y , z , w , and v_i are the oxidation numbers of glucose, oxygen, biomass, CO₂, and metabolites, respectively.

Table III. Carbon balance of Vhb-producing *E. coli* (after 31 h of cultivation).

Vhb (μmol/g DCW)	Carbon balance (mmol carbon)						Recovery (%)
	Glucose ^a	Biomass ^b	Σ(Metabolites) ^c	CO ₂ (off gas)	O ₂ (off gas)	CO ₂ (redox bal.)	
0	271	20.4	178	57.0	66.0	58.3	94
0.5	281	27.2	158	76.9	86.7	82.5	93
1.2	290	31.6	173	74.6	84.6	79.6	96
2.3	341	38.7	207	81.4	88.6	82.4	96
3.4	333	41.8	185	83.3	94.9	93.7	93
3.8	333	45.7	201	91.5	100.0	98.8	102

^aInitial glucose concentration of 4 g/L plus 0.25 g/h of feeding after culture A₆₀₀ 1.5 and 0.5 g/h after A₆₀₀ 3.0.

^bBased on 39.8 mmol carbon/g DCW.

^cSum of excreted acetate, ethanol, formate, succinate, D-lactate, and pyruvate in mmol carbon.

The average oxidation state of cellular carbon (z) was estimated to be -0.20 based on the oxidation of nitrogen and the reduction of sulfur that occur in cells grown in minimal media containing NH_4^+ and SO_4^{2-} .¹³ Using the method described in Neidhardt et al.,²⁴ the other oxidation numbers were calculated to be as follows: x , 0; y , -4 ; w , $+4$; v_{acetate} , 0; v_{ethanol} , -2 ; v_{formate} , 1; $v_{\text{succinate}}$, 1; v_{lactate} , 0. The amount of oxygen consumed (in millimoles) was determined from exhaust gas measurement.

The theoretical CO_2 production was calculated from Equation (1) and compared with CO_2 evolution from exhaust gas measurement (Table III). Analysis showed that all CERs calculated from the redox balance of the different IPTG-induced cultures, except one, were within 93% or higher of the measured CO_2 . Results of carbon and redox balances indicate that our CER measurements were accurate and that our findings of improved growth yield and suppressed by-product excretion by VHb of microaerobic *E. coli* are correct.

Effect of VHb Levels on Metabolic Flux Distribution

Reduction of by-product formation indicates altered carbon metabolism. To gain insight on the effect of VHb on the flux distribution within central carbon metabolism, a metabolic flux analysis was performed on these cultures. The theory behind such analysis has been described extensively elsewhere^{11,32-34}; therefore only the principle will be summarized below. Metabolic flux analysis enables one to estimate the carbon flow through metabolic pathways by solving mass balances on pertinent precursor metabolites. To construct a suitable metabolic map for flux distribution elucidation, the biochemistry of the metabolic reactions is first systematically incorporated. Then a metabolic quasi-steady state (QSS), in which the sum of the fluxes involved in the formation and degradation of a metabolite equals zero, is assumed (see Vallino and Stephanopoulos³³ for a discussion of the validity of this assumption in this context). The metabolic flux distribution within the network is then calculated from the following system of equations:

$$S \cdot v = b \quad (2)$$

where S is a matrix consisting of stoichiometric coefficients from the metabolic map, v is a vector of unknown metabolic fluxes, and b is a vector of known fluxes for measurable metabolite synthesis and for biomass formation.

In our analysis, the reaction network was constructed primarily from established biochemistry in the literature⁹; included in this network were fluxes that lead to and depart from precursor metabolites that appear in the glycolytic pathway, the pentose phosphate pathway, and the tricarboxylic acid (TCA) cycle. In addition, the anaplerotic reaction catalyzed by phosphoenolpyruvate carboxylase for the conversion of phosphoenolpyruvate to oxaloacetate and the reaction catalyzed by pyruvate-formate lyase for the conver-

sion of pyruvate to formate were included in the network of reactions.

Fluxes leading to precursors for heme biosynthesis (to account for VHb) were insignificant (in $\mu\text{mol/g DCW/h}$) compared to typical catabolic fluxes (in mmol/g DCW/h) and were not included. The extra protein synthesis capacity needed for VHb expression was lumped into precursor metabolite fluxes to biosynthesis. The reaction network also contained carbon dioxide and NAD(P)H ($\text{NADH} + \text{NADPH}$) mass balances, which utilize information from the off-gas measurement. Fluxes for ATP generation and for NADH/NADPH interconversion catalyzed by NADH transhydrogenase, which are coupled with the reaction network, were calculated after Equation (2) was solved. The solution to Equation (2) was determined using a constrained least-square approach in which the objective was to minimize the sum of the squares of the residuals of the metabolite mass balances. The least-square problem was solved subject to a set of constraints which demanded positive fluxes for the irreversible steps and positive net flux of reducing equivalents. The Appendix presents the set of mass balance equations from which S , v , and b were constructed, the constraints, and a metabolic map which details the location of all the reactions.

The effect of VHb dosage on *E. coli* carbon flux distribution was analyzed using parameters measured during the late exponential growth phase (between hours 13 and 19) of the six glucose fed-batch cultivations (Fig. 2A). Flux to biosynthesis from each precursor metabolite was derived by multiplying the specific growth rate of cells by the molar requirement of each precursor for synthesis of 1 g biomass.²⁴ Fluxes to extracellular metabolite excretions were obtained by dividing the rate of metabolite accumulation by the cell density. Metabolite fluxes are expressed in mmol/g DCW/h and listed in Table IV. Similar to our findings in the late fed-batch phase of cultivation, VHb has a negative effect on by-product formation during the exponential phase, although by a smaller magnitude than that during the late fed-batch phase (Table II). Increasing VHb concentrations monotonically decreased the accumulation rates of all but one metabolite, from a maximal reduction of 35% in ethanol and succinate to 25% in formate and lactate. VHb did not appear to affect acetate flux during exponential phase since acetate accumulation rates of different cultures fluctuated around a mean. Table IV also shows that at least 95% of the carbon influx was recovered in the form of biomass, CO_2 , and by-product fluxes from all six cultivations.

Based on random initialization of the nonlinear optimization problem, the minimum sum-of-residuals-squared solution to Equation (2) was found for all six strains; the sum of the squares of the residuals was on the order of 10^{-3} – 10^{-2} in all cases. The flux distributions of the uninduced, VHb-free control and the highest VHb-expressing cultures normalized to a same glucose consumption rate of 2.6 mmol/g DCW/h are presented in Figure 3. A first inspection of these flux distributions confirms the biochemical and

Table IV. Carbon flux of Vhb-producing *E. coli* (in exponential phase, 13–19 h).

Vhb ($\mu\text{mol/g DCW}$)	Carbon flux ^a								Recovery (%)
	mmol carbon/g DCW h			mmol/g DCW h					
	Gluc	Biomass ^b	CO ₂	Acet	ETOH	Form	D-Lac	Suc	
0	15.7	4.8	2.2	1.1	0.43	3.7	0.22	0.20	98
0.5	16.4	5.1	1.8	1.6	0.38	3.5	0.32	0.19	97
1.2	15.7	5.3	2.0	1.2	0.32	3.2	0.27	0.16	95
2.3	14.8	5.7	1.9	1.0	0.34	2.8	0.18	0.13	95
3.4	16.1	6.6	1.8	1.4	0.30	3.0	0.19	0.13	98
3.8	15.4	6.4	1.5	1.4	0.28	2.8	0.16	0.12	97

^aFlux calculated from $\mu(dm/dt)/(dx/dt)$, where m denotes metabolite and x biomass.

^bCalculated from $Q_{\text{gluc}}Y_{x/\text{gluc}}$.

thermodynamic reasonability of the model, since no irreversible reactions exhibit negative fluxes. Our model also indicates that the conversion of pyruvate to acetyl coenzyme A is catalyzed by pyruvate–formate lyase and not by pyruvate dehydrogenase, as the calculated flux from pyruvate dehydrogenase amounted to zero.

Examination of the overall flux distributions revealed two dramatic differences between the control and the Vhb-expressing cultures. In the presence of Vhb, fluxes through the pentose phosphate pathway are increased and, as a result, fluxes through the Embden–Meyerhof–Parnas pathway are decreased. Fluxes entering the TCA cycle are also decreased with Vhb expression. Comparing the two cases shown in Figure 3, the percentage of glucose that enters the pentose phosphate pathway, calculated by dividing f_1 by the sum of f_{glucose} , $-f_3$, and f_6 , is 0% for the uninduced W3110:pKTV1 culture and 45% for the induced culture. This increase is possibly due to an increased demand for NADPH of Vhb⁺ cells as consequences of increased biosynthesis and decreased TCA flux.

The effect of Vhb on fluxes leading to the TCA cycle can be studied by examining changes in the split ratios of carbon flux at important branch points, or nodes.³⁰ The oxaloacetate (OAA) branch split ratio at the phosphoenolpyruvate (PEP) node, calculated by taking the ratio of f_{11} and f_9 (Fig. 3), are 14% and 19% for the uninduced Vhb-free control and the highest Vhb dose cells, respectively. The isocitrate (Iso-Cit) branch split ratio at the acetyl coenzyme A (AcCOA) node, the ratio of f_{13} and f_{formate} , is 43% for the control and 18% for the Vhb⁺ cells.

To check whether Vhb dosage exerts a trend on the flexibility of the PEP and AcCOA nodes, we compared the split-ratios of these nodes under different Vhb expression levels. Tables V and VI present the flux distributions and the split-ratios at the PEP and AcCOA nodes, respectively, for the six cultivations. The location of each flux can be found in Figure 3. Results show that, in comparison to AcCOA, the node at PEP is more rigid with respect to Vhb concentration: the OAA-branch split-ratio at PEP remains relatively unaffected between 14% and 19%. The node at AcCOA, on the other hand, is more flexible under high Vhb concentrations. The IsoCit-branch split-ratio at AcCOA

stays high around 34% with increasing Vhb levels up to 2.3 $\mu\text{mol/g DCW}$, but the ratio drops to 22% and 18% with 3.4 $\mu\text{mol/g DCW}$ and 3.8 $\mu\text{mol/g DCW}$ of Vhb, respectively. This analysis suggests that attempts to modify enzymatic activities at PEP are unlikely to bring changes in the fraction of carbon channeled to the TCA cycle at any Vhb concentration.

In contrast, the AcCOA node, which is flexible at high Vhb levels, might be explored for possibilities of enzymatic modifications if a changed TCA flux is desired. Table VI also indicates that the fraction of fluxes to the pentose phosphate pathway increases with increasing Vhb concentration from 14% with 0.5 $\mu\text{mol Vhb/g DCW}$ to 45% with 3.8 $\mu\text{mol Vhb/g DCW}$.

With a higher oxygen uptake rate, Vhb-synthesizing cells can recycle NADH to NAD⁺ faster than the control cells, and the results show a respiratory-derived NAD⁺ flux of 5.46 mmol/g DCW/h for the 3.8 $\mu\text{mol Vhb/g DCW}$ culture and 3.38 mmol/g DCW/h for the Vhb-cells. From the flux distribution analysis the activity of the NADH transhydrogenase can also be estimated. The rate of NADPH→NADH conversion by the transhydrogenase shows an inverse relationship with Vhb concentration; the cells without Vhb afford a NADPH flux of 0.6 mmol/g DCW/h while the cells with the highest Vhb concentration generate 0.85 mmol/g DCW/h of NADH. The overall NAD(P)H balance reveals a higher NAD(P)H flux (f_{16}) for the uninduced, Vhb-free cells than for the Vhb-containing cells (2.68 vs. 0 mmol/g DCW/h; in Fig. 3). This indicates that cells are under a more oxidized state in the presence of Vhb.

Unexpectedly, cells synthesizing Vhb produce less ATP from substrate-level phosphorylation than the control, Vhb-free cells (f_{ATPsp} ; Table V). However, the ATP synthesis rate from oxidative phosphorylation, calculated from the oxygen consumption rate and assuming a P/O ratio of 2, compensates for this deficiency. As a result, cells with Vhb afford on the average a 13% higher net (reaction network plus respiration) ATP flux ($f_{\text{ATPoverall}}$) than the control cells (12.7 vs. 11.2 mmol/g DCW/h; Table V). The calculated values for $f_{\text{ATPoverall}}$ may seem high, but we did not consider in the analysis futile cycles and slippage

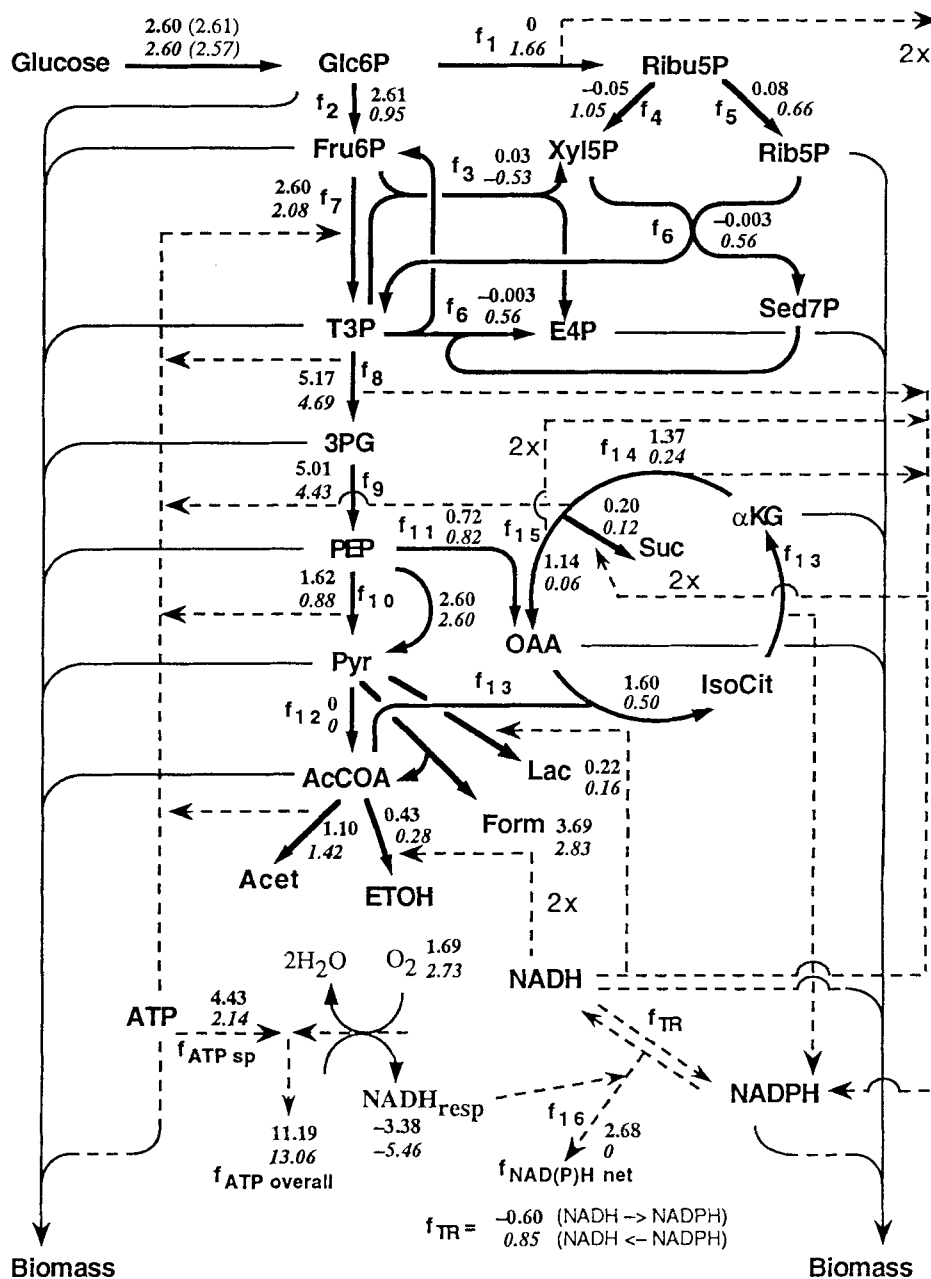


Figure 3. Metabolic map for glucose fed-batch cultivations during exponential growth phase (between hours 13 and 19 of fermentation). Fluxes from cultures without Vhb (plain numbers) and with 3.8 μmol Vhb/g DCW (italic numbers) are shown. Fluxes (in mmol/g DCW/h) were normalized to a same glucose consumption rate of 2.60 mmol/g DCW h. The actual glucose uptake rates are shown in parentheses. Fluxes of cells with other Vhb concentrations are summarized in Table V.

or leakage of protons from the cytoplasmic membrane which might very well claim a large portion of the estimated overall ATP fluxes. Moreover, these values have been calculated for a P/O ratio of 2. In general this ratio is lower, and for microaerobic conditions it is much lower than 2. However, if we assume the same P/O ratio for each strain, the conclusion that Vhb has a positive effect on the net ATP flux still holds.

Prior metabolic flux analysis of *E. coli* have compared the thermodynamic efficiencies of growth of different sys-

tems based upon the net [2H] production in the central carbon metabolic pathways (this quantity is, in the notation used here, equal to $2f_1 + f_8 + f_{12} + f_{13} + f_{14} + 2f_{15} - 2f_j - f_j$).¹¹ Evaluation of the quantity for the Vhb⁻ culture gives 9.34 mol [2H]/g DCW/h and 8.15 mol [2H]/g DCW/h for the culture maximally induced for Vhb expression. A smaller value indicates that these cells require less reducing power to generate the same amount of biomass, or, in other words, exhibit an increased thermodynamic efficiency of growth.

Table V. Summary of flux distribution of VHb-producing *E. coli*.

Fluxes ^a (mmol/g DCW h)	W3110:pKTV1 with different VHb (μmol/g DCW)					
	0	0.5	1.2	2.3	3.4	3.8
f_{glc}	2.60	2.60	2.60	2.60	2.60	2.60
f_{acet}	1.10	1.52	1.19	1.05	1.36	1.42
f_{ETOH}	0.43	0.36	0.32	0.36	0.29	0.28
f_{form}	3.69	3.32	3.18	2.95	2.91	2.83
f_{lac}	0.22	0.30	0.27	0.19	0.18	0.16
f_{suc}	0.20	0.18	0.16	0.14	0.13	0.12
f_1	0	0.4	0.61	1.06	1.35	1.66
f_2	2.61	2.18	1.97	1.51	1.25	0.95
f_3	0.03	-0.07	-0.13	-0.27	-0.40	-0.53
f_4	0.05	0.18	0.31	0.60	0.81	1.05
f_5	0.08	0.22	0.30	0.46	0.56	0.66
f_6	-0.003	0.11	0.18	0.33	0.44	0.56
f_7	2.60	2.36	2.26	2.10	2.10	2.08
f_8	5.17	4.78	4.64	4.45	4.58	4.69
f_9	5.01	4.60	4.44	4.23	4.33	4.43
f_{10}	1.62	1.38	1.22	0.94	0.96	0.88
f_{11}	0.72	0.53	0.53	0.56	0.66	0.82
f_{12}	0	0	0	0	0	0
f_{13}	1.60	0.98	1.19	0.99	0.64	0.50
f_{14}	1.37	0.85	1.04	0.83	0.44	0.24
f_{15}	1.14	0.68	0.88	0.69	0.30	0.06
f_{16}	2.68	0.70	0.87	1.09	0	0
$f_{\text{ATP sp}}^b$	4.43	3.94	3.37	2.39	2.26	2.14
$f_{\text{ATP overall}}^c$	11.19	12.30	13.29	11.70	12.74	13.06
$f_{\text{NADH resp}}^d$	-3.38	-4.18	-4.96	-4.64	-5.24	-5.46
f_{TR}^e	-0.6	-0.42	-0.01	0.37	0.41	0.85

^aFluxes were normalized to a same specific glucose uptake rate of 2.60 mmol/g DCW h (from Table I).

^bNet ATP flux from substrate level phosphorylation.

^c $f_{\text{ATP overall}} = f_{\text{ATP sp}} + f_{\text{ATP respiration}}$. A P/O of 2.0 was assumed.

^dNADH flux from the electron transport chain was calculated by multiplying Q_{O_2} by 2. Negative flux denotes generation of NAD from NADH.

^eNADH synthesis by the NADPH/NADH transhydrogenase.

DISCUSSION

In this study we have demonstrated that, by modulating the synthesis of VHb over a wide range from zero to a level comparable to expression from high-copy-number plasmids, cell growth was improved and by-product excretion was reduced with increasing VHb concentrations. Satur-

tion of growth improvement due to VHb was readily observed from VHb concentration profiles of final cell density and specific oxygen consumption rate, which show that beyond 3.4 μmol VHb/g DCW, only marginal enhancements of these qualities were obtained. A metabolic distribution analysis revealed increasing VHb expression changed flux patterns to the pentose phosphate, TCA, NADH, and ATP pathways.

The finding that VHb decreases *E. coli* by-product formation has implication for the oxidation–reduction and energetic state of cells under microaerobic conditions. Indeed, fermentative pathways for production of reduced metabolites are coupled with synthesis of ATP and/or oxidation of reducing equivalent/NADH. Formation of ethanol and succinate result in production of 2 mol NAD⁺/mol metabolite. Lactate fermentation recycles 1 NADH to NAD⁺. Synthesis of acetate, although coupled to generation of 1 NADH, provides one molecule of ATP per molecule of acetate. The fact that *E. coli* grown under our experimental scheme produced large quantities of by-products indicates that cells were under heavily reduced conditions and were seeking a redox sink in the form of reduced metabolites.

The observation that the presence of VHb greatly de-

Table VI. Effect of VHb levels on flux ratios.^a

VHb (μmol/g DCW)	% PPP ^b	% OAA ^c at PEP	% IsoCit ^d at AcCoA
0	0	14	43
0.5	14	12	30
1.2	21	12	37
2.3	33	13	34
3.4	39	15	22
3.8	45	19	18

^aLocation of the fluxes is shown in Fig. 3.

^bPercentage of carbon through the pentose phosphate pathway: $f_1/(f_{\text{glucose}} - f_3 + f_6)$.

^cOxaloacetate branch split ratio at phosphoenolpyruvate: f_{11}/f_9 .

^dIsocitrate branch split ratio at acetyl coenzyme A: $f_{13}/(f_{12} + f_{\text{formate}})$.

pressed the formation of ethanol and succinate by more than 50% relative to the control suggests that Vhb⁺ cells could regenerate somewhere else the reducing equivalents that would otherwise originate from by-product synthesis. Indeed, our off-gas measurement showed an enhanced respiratory activity from Vhb-synthesizing cells which suggest a higher turnover rate of NADH to NAD⁺ for the Vhb⁺ cells. The metabolic flux distribution analysis also indicated that the Vhb⁻ cells are under a more reduced state by affording a net positive NAD(P)H flux while those of Vhb⁺ cells produce smaller and, in some cases, zero NADH(P)H fluxes. This is similar to our previous observation from culture fluorescence measurement of cells subjected to diminishing oxygen transients.³¹

A decrease in acetate excretion and an increase in growth yield on glucose from Vhb-expressing *E. coli* imply that cells are more competent in providing ATP in the presence of Vhb, possibly through a more active and/or efficient oxidative phosphorylation pathway. Our metabolic flux analysis indicates that Vhb-producing cells synthesize a smaller ATP flux from substrate-level phosphorylation than the Vhb⁻ cells and rely on the oxidative phosphorylation pathway as a major contributor in energy synthesis. With a more active respiratory pathway, Vhb producers can support a higher ATP synthesis rate. This analysis is consistent with a nuclear magnetic resonance (NMR) study which demonstrated a higher ATP synthesis rate for the Vhb-expressing *E. coli* over its isogenic control.⁵

Judging from the growth patterns (Fig. 2A), Vhb appears to play a role in prolonging cell growth during oxygen-limited conditions. Without Vhb, cells ceased to grow after the end of exponential phase. The higher the Vhb concentration, the longer the growth was sustained. Cells with the highest Vhb concentration continued to grow beyond the endpoint of investigation. Suppressed by-product synthesis and enhanced respiration observed in Vhb-expressing cells resemble characteristics of cells growing under elevated DO tensions. Our experimental data suggest that the degree of ‘oxygenation’ in Vhb-expressing cultures increases with increasing Vhb concentrations until a saturation level is attained. In a metabolic performance optimization study in which the flux distributions under different dissolved oxygen tensions were computed with the objective of optimal growth rate, Varma et al.³⁴ showed that the percentage of glucose entering the pentose phosphate pathway increases with increasing oxygenation rates, from 2% under anaerobic conditions to 15% with 7 mmol O₂/g DCW/h and to 45% with 12 mmol O₂/g DCW/h. Coincidentally, our metabolic distribution analysis also reveals a more active pentose phosphate pathway under increasing Vhb concentrations. A proposed mechanism of Vhb action in enhancing intracellular effective dissolved oxygen tension by providing additional oxygen to the terminal oxidases of *E. coli* has been discussed elsewhere.¹⁴

The finding of Vhb perturbs the flux distribution of central carbon metabolism in addition to the previously reported enhancements in microaerobic respiratory pathway suggests new perspectives for the application of Vhb. The

pentose phosphate pathway is important, not only for its function in generation of NADPH as reducing agent for biosynthesis, but also in the production of precursors for aromatic amino acid synthesis. An increase in the flow of carbon through the pentose phosphate pathway by Vhb might affect key enzymes and enhance synthesis of aromatic amino acids. In contrast, the predicted decrease in fluxes through oxaloacetate and α -ketoglutarate, which serve as precursor metabolites for 10 amino acids, may discourage cloning of Vhb for the sole purpose of improving yields of TCA derived amino acids.

This research was supported by the Swiss Priority Program in Biotechnology. The authors are grateful to H. Holms for his helpful suggestions on flux distribution analysis.

NOMENCLATURE

Glc6	glucose-6-phosphate
Ribu5P	ribulose-5-phosphate
Xyl15P	xylulose-5-phosphate
Rib5P	ribose-5-phosphate
Fru6P	fructose-6-phosphate
T3P	triose-3-phosphate
E4P	erythrose-4-phosphate
Sed7P	sedoheptulose-7-phosphate
3PG	3-phosphoglycerate
PEP	phosphoenolpyruvate
Pyr	pyruvate
AcCoA	acetyl coenzyme A
OAA	oxaloacetate
α KG	α -ketoglutarate
IsoCit	isocitrate
Suc	succinate
Form	formate
ETOH	ethanol
Acet	acetate
Lac	lactate

APPENDIX

This appendix contains the mass balances and the flux distribution map used to construct the metabolic network of *E. coli* W3110:pKTV1.

Metabolite Flux Vector

A constrained least-square approach was applied to estimate the fluxes from the following mass balances. The objective of this approach was to minimize the sum of the squares of the residuals of the metabolite mass balances. The constraints applied were positive fluxes for the irreversible reactions and positive net flux of reducing equivalents. Location of each flux can be found in the accompanying metabolic map (Fig. A1). Fluxes with numeral subscripts denote unknown fluxes, and fluxes with letter subscripts denote either measurable fluxes or biosynthesis fluxes calculated from the biomass synthesis requirements of each precursor metabolite. In addition, f_{CO_2} and f_{O_2} are the carbon dioxide evolution rate and the oxygen uptake rate, respectively, measured from the off-gas. Here, f_{TR} , is the net

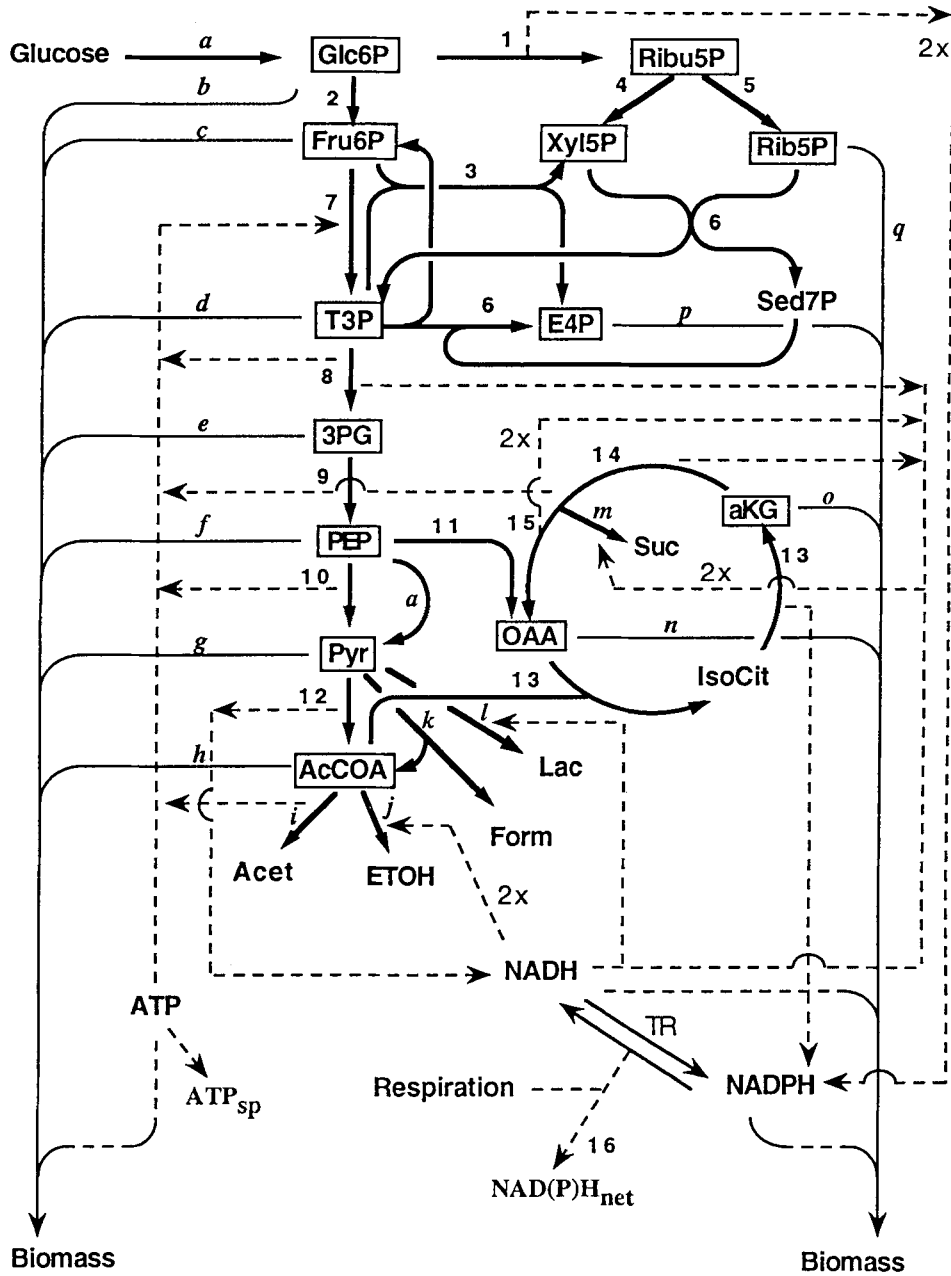


Figure A1. Flux distribution map.

NADH flux from NADPH/NADH transhydrogenase and $f_{ATP_{sp}}$ is the net ATP flux from substrate level phosphorylation.

Mass balances:

$$\begin{aligned}
 1. \text{ Glc6-P: } & f_a - f_b - f_2 - f_1 = 0 \\
 2. \text{ Rib5P: } & f_1 - f_5 - f_4 = 0 \\
 3. \text{ Xyl5P: } & f_4 + f_3 - f_6 = 0 \\
 4. \text{ Rib5P: } & f_5 - f_q - f_6 = 0 \\
 5. \text{ Fru6P: } & f_2 - f_c - f_7 - f_3 + f_6 = 0 \\
 6. \text{ T3P: } & 2f_7 - f_d - f_8 - f_3 + f_6 - f_6 \\
 & = 0 \\
 7. \text{ E4P: } & f_3 + f_6 - f_p = 0 \\
 8. \text{ 3PG: } & f_8 - f_e - f_9 = 0
 \end{aligned}$$

$$\begin{aligned}
 9. \text{ PEP: } & f_9 - f_f - f_{11} - f_a - f_{10} \\
 & = 10 \\
 10. \text{ Pyr: } & f_{10} - f_g - f_a - f_{12} - f_k \\
 & - f_l = 0 \\
 11. \text{ AcCOA: } & f_{12} - f_h - f_i - f_j + f_k \\
 & - f_{13} = 0 \\
 12. \text{ OAA: } & f_{11} + f_{15} - f_{13} - f_n = 0 \\
 13. \text{ aKG: } & f_{13} - f_{14} - f_o = 0 \\
 14. \text{ Suc: } & f_{14} - f_{15} - f_m = 0 \\
 15. \text{ CO}_2: & f_1 - f_{11} + f_{12} + f_{13} + f_{14} \\
 & - f_{CO_2} = 0 \\
 16. \text{ NADH } & 2f_1 + f_8 + f_{12} + f_{13} + f_{14} \\
 & + 2f_{15} - f_{16} - 2f_{O_2} \\
 \text{NADPH: } & -f_{biosyn/nadh} \\
 & - f_{biosyn/nadh} = 0
 \end{aligned}$$

Constraints:

$$f_1 \geq 0 \quad f_7 \geq 0 \quad f_{10} \geq 0 \quad f_{12} \geq 0 \quad f_{16} \geq 0$$

NAD(P)H transhydrogenase (f_{TR}):

$$2f_1 + f_{13} - f_{\text{biosyn/nadp}} = f_{TR}$$

ATP:

$$f_8 + f_{10} - f_7 + f_i + f_{14} - f_{\text{biosyn/atp}} = f_{\text{ATP}_p}$$

References

1. Bachmann, B. J. 1987. Derivations and genotypes of some mutant derivatives of *Escherichia coli* K-12. pp. 1191–1219. In: J. L. Ingraham, K. B. Low, B. Magasanik, M. Schaechter, and H. E. Umbarger (eds.), *Escherichia coli* and *Salmonella typhimurium*: Cellular and molecular biology. American Society for Microbiology, Washington, D.C.
2. Bergmeyer, H. U. 1985. In: Methods of enzymatic analysis, vol. VI. VCH Publishers, Deerfield Beach, FL.
3. Bergmeyer, H. U. 1985. In: Methods of enzymatic analysis, vol. VII. VCH Publishers, Deerfield Beach, FL.
4. Bolivar, F., Rodriguez, R. L., Greene, P. J., Betlach, M. C., Heyneker, H. L., Boyer, H. W., Cross, J. H., Falkow, S. 1977. Construction and characterization of new cloning vehicles. II. A multipurpose cloning system. *Gene* 2: 95–113.
5. Chen, R., Bailey, J. E. 1994. Energetic effect of *Vitreoscilla* hemoglobin expression in *Escherichia coli*: An on-line ^{31}P NMR and saturation transfer study. *Biotechnol. Prog.* 10: 360–364.
6. Delacruz, N., Payne, G. F., Smith, J. M., Coppella, S. J. 1992. Bioprocess development to improve foreign protein production from recombinant *Streptomyces*. *Biotechnol. Biotechnol.* 8: 307–315.
7. DeModena, J. A., Gutierrez, S., Velasco, J., Fernandez, F. J., Fachine, R. A., Galazzo, J. L., Hughes, D. E., Martin, J. F. 1993. The production of cephalosporin C by *Acremonium chrysogenum* is improved by the intracellular expression of a bacterial hemoglobin. *Bio/Technology* 11: 926–929.
8. Galazzo, J., Bailey, J. E. 1990. Fermentation pathway kinetics and metabolic flux control in suspended and immobilized *Saccharomyces cerevisiae*. *Enz. Microb. Technol.* 12: 162–172.
9. Gottschalk, G. 1986. *Bacterial metabolism*, 2nd edition. Springer-Verlag, New York.
10. Hart, R. A., Bailey, J. E. 1991. Purification and aqueous 2-phase partitioning properties of recombinant *Vitreoscilla* hemoglobin. *Enz. Microb. Technol.* 13: 788–795.
11. Holms, W. H. 1986. The central metabolic pathways of *Escherichia coli*: Relationship between flux and control at a branch point, efficiency of conversion to biomass, and excretion of acetate. pp. 69–105. In: *Current topics in cellular regulation*, vol. 28. Academic New York.
12. Iuchi, S., Lin, E. C. C. 1991. Adaptation of *Escherichia coli* to respiratory conditions: Regulation of gene expression. *Cell* 66: 5–7.
13. Jensen, P. R., Michelsen, O. 1992. Carbon and energy metabolism of *atp* mutants of *Escherichia coli*. *J. Bacteriol.* 174: 7635–7641.
14. Kallio, P. T., Kim, D. J., Tsai, P. S., Bailey, J. E. 1994. Intracellular expression of *Vitreoscilla* hemoglobin alters *Escherichia coli* energy metabolism under oxygen-limited conditions. *Eur. J. Biochem.* 219: 201–208.
15. Khosla, C., Bailey, J. E. 1988. Heterologous expression of a bacterial haemoglobin improves the growth properties of recombinant *Escherichia coli*. *Nature* 331: 633–635.
16. Khosla, C., Bailey, J. E. 1989. Evidence for partial export of *Vitreoscilla* hemoglobin into the periplasmic space in *Escherichia coli*. *J. Mol. Biol.* 210: 79–90.
17. Khosla, C., Curtis, J. E., DeModena, J., Rinas, R., Bailey, J. E. 1990. Expression of intracellular hemoglobin improves protein synthesis in oxygen-limited *Escherichia coli*. *Bio/Technol.* 8: 849–853.
18. Khosravi, M., Webster, D. A., Start, B. C. 1990. Presence of bacterial hemoglobin gene improves α -amylase production of a recombinant *Escherichia coli* strain. *Plasmid* 24: 190–194.
19. Konstantinov, K. B., Nishio, N., Seki, T., Yoshida, T. 1991. Physiologically motivated strategies for control of the fed-batch cultivation of recombinant *Escherichia coli* for phenylalanine production. *J. Ferm. Bioeng* 71: 350–355.
20. Laemmli, U. K. 1970. Cleavage of structural proteins during the assembly of the head of bacteriophage T4. *Nature* 227: 680–685.
21. Magnolo, S. K., Leenutaphong, D. L., DeModena, J. A., Curtis, J. E., Bailey, J. E., Galazzo, J. L., Hughes, D. E. 1991. Actinorhodin production by *Streptomyces coelicolor* and growth of *Streptomyces lividans* are improved by the expression of a bacterial hemoglobin. *Bio/Technology* 9: 473–476.
22. Manfredini, R., Cavallera, V., Marini, L., Donati, G. 1983. Mixing and oxygen transfer in conventional stirred fermentors. *Biotechnol. Bioeng.* 25: 3115–3131.
23. Neidhardt, F. 1987. Chemical composition of *Escherichia coli*. pp. 4–6. In: J. L. Ingraham, K. B. Low, B. Magasanik, M. Schaechter, and H. E. Umbarger (eds.), *Escherichia coli* and *Salmonella typhimurium*: Cellular and molecular biology. American Society for Microbiology, Washington, DC.
24. Neidhardt, F. C., Ingraham, J. L., Schaechter, M. 1990. Biosynthesis and fueling. pp. 133–173. In: *Physiology of the bacterial cell: A molecular approach*. Sinauer Associates, Sunderland, MA.
25. O'Connor, G. M., Sanchezriera, F., Cooney, C. L. 1992. Design and evaluation of control strategies for high cell-density fermentations. *Biotechnol. Bioeng.* 39: 293–304.
26. Onken, U., Leifke, E. 1989. Effect of total and partial pressure (oxygen and carbon dioxide) on aerobic microbial processes. *Adv. Biochem. Eng. Biotechnol.* 40: 137–169.
27. Oosterhuis, N. M. G., Kossen, N. W. F. 1984. Dissolved oxygen concentration profiles in a production scale bioreactor. *Biotechnol. Bioeng.* 26: 546–555.
28. Papoutsakis, E. T., Meyer, C. L. 1985. Equations and calculations of product yields and preferred pathways for butanediol and mixed-acid fermentation. *Biotechnol. Bioeng.* 27: 50–66.
29. Spiro, S., Guest, J. R. 1991. Adaptive responses to oxygen limitation in *Escherichia coli*. *Trends in Biochem. Sci.* 16: 310–314.
30. Stephanopoulos, G., Vallino, J. J. 1991. Network rigidity and metabolic engineering in metabolic overproduction. *Science* 252: 1675–1681.
31. Tsai, P. S., Rao, G., Bailey, J. E. Improvement of *Escherichia coli* microaerobic oxygen metabolism by *Vitreoscilla* hemoglobin: New insights from NAD(P)H fluorescence and culture redox potential. *Biotechnol. Bioeng.*
32. Vallino, J., Stephanopoulos, G. 1990. Flux determination in cellular bioreaction network: Application to lysine fermentation. pp. 205–219. In: *Frontiers in bioprocessing*. CRC Press, Boca Raton, FL.
33. Vallino, J., Stephanopoulos, G. 1993. Metabolic flux distributions in *Corynebacterium glutamicum* during growth and lysine overproduction. *Biotechnol. Bioeng.* 41: 633–646.
34. Varma, A., Boesch, B., Palsson, B. O. 1993. Stoichiometric interpretation of *Escherichia coli* glucose catabolism under various oxygenation rates. *Appl. Environ. Microbiol.* 59: 2465–2473.
35. Varma, A., Palsson, B. O. 1994. Metabolic flux balancing: Basic concepts, scientific and practical use. *Bio/Technology* 12: 994–998.
36. Winston, S. E., Fuller, S. A., Hurrell, J. G. R. 1987. Western blotting. pp. 10.8.1–10.8.6. In: F. M. Ausubel, R. Brent, R. E. Kingston, D. D. Moore, J. G. Seidman, J. A. Smith, and K. Struhl (eds.), *Current protocols in molecular biology*. Wiley, New York.